Investigation in the Effect of Applied Voltage and Working Pressure on Some Plasma Parameters in the Positive Column of Dc Glow Discharge

Mustafa K. Jassim

Department of Physics, College of Education for Pure Sciences Ibn Al-Haitham, University of Baghdad, Baghdad, Iraq

Email: qqqqq1961@gmail.com

Abstarct

Comsol multiphysics software is established to make a simulation that is comparable with experimental device. by utilizing comsol, the positive column domain of direct-current glow discharge with argon is considered for both of different applied voltage and working gas pressure. The calculations are exhibited by using a precise collision cross sections and Townsend coefficients for the argon. The impacts of voltage and pressure on the Debye length, number of particles in Debye sphere and plasma frequency are calculated and graphically delineated. With this regard to the dependence of plasma parameters on the applied voltage and pressure, some of them are found to be compatible with the experimental results, while others are not. For example, the calculations of the COMSOL shows that the electron temperature is not always decreasing with the increase in the applied voltage, and the Debye length does not give a linearly decreasing relationship but rather an exponentially decreasing relationship. Also, the calculations do not reproduce and match the experimental results for the dependence electron density on working pressure at various potentials.

Keywords: COMSOL Multiphysics, dc glow discharge, Plasma density, Electron temperature, Plasma frequency, Argon.

1. Introduction

For a long time ago and still to nowadays the low-pressure glow discharge is used for fluorescent lamps, neon light, plasma-screen TV, and treatment of material and gas lasers [1-4]. The discharge is a kind of ionized gas or plasma formed by applying the electric potential difference between two electrodes in a glass tube containing a low-pressure a reactive gas or inert gas [5]. A slight fraction of gas atoms at first are ionized by thermal collisions among atoms. The electrons are emitted from the cathode and accelerated away towards anode due to the potential difference between the electrodes. This process gives rise to collisions with the gas atoms and generates electron-ion pairs on their way through collisions with neutral atoms and ionizes them. The ions are driven in the opposite direction by the same potential. The generated ions move in the opposite direction, striking the cathode and new electrons are

emitted. Although, the created plasma between the electrodes depends on the degree of ionization, the emission of secondary electrons at the cathode is responsible for preserving the discharge [6]. Secondary electron emission is resulting from particle impacts on the surface of the electrode. The particles may be positive ions excited atoms, photons and electron [7]. The discharge glows with a coloured light depending on excitation collisions which gives rise to excited species [8]. The excited species decay to lower levels by the emission of light that depends on a type of the used gas. The glow discharge is used in plasma physics and analytical chemistry because the light produced can reveal information about the atomic interactions in the gas [9]. In addition to that the DC discharge is used in sputtering for surface [10]. In science there needs to be consistency between theory and experiment. This means that what is done experimentally has basically a theoretical basis. The accomplishment of the simulation of a certain phenomenon is thought to indicate what would happen if applied through an experiment. There are rather a few theoretical and experimental researches on the phenomenon of glow electrical discharge. Some of these researches discusses the effect of working pressure and applied voltages on these devices [11-14]. In this research we proceed to explore the extent to which experimental results are consistent with simulation of the phenomenon using COMSOL Multiphysics program. The program is Finite Element Modelling software [15]. Several plasma parameters will be taken out in the positive column of glow discharge by change working pressure and applied potential. The discharge composes of two parallel rectangle electric poles; anode and cathode supposed being made of stainless steel of width 3.75 cm and separated at a distance of 37.4 cm. The cathode is grounded while the anode is powered and associated with an external circle. The discharge contains inside a chamber filled with argon gas at various pressures. The calculations are accomplished at constantly reduced electron mobility and with work function value of the stainless steel electrodes. In the COMSOL Multiphysics, the species are organized based on the chemistry of plasma. The plasma chemistry is determined by a group of volumetric reactions, electron impact, and surface reactions. Furthermore, boundary conditions for electrons and the electric potential are included. Argon is considered the most straightforward mechanisms to actualize at low pressures [16]. Further, we acquire to assign complete cross section data so as to model the processes included such as elastic and excitation, ionization, and metastable quenching. **Table 1 and 2,** demonstrates the utilized reactions in the simulation which is the predominant reaction in the two gas phase and surface phase. The electronically excited states can be collected into single species which brings about a chemical mechanism comprising of just three species and seven reactions.

Table 1. Collisions and reactions 11odeled.

Type	Reaction	$\Delta\varepsilon(\mathbf{eV})$
Elastic	$e + Ar \Rightarrow e + Ar$	0
Excitation	$e + Ar \Rightarrow e + Ars$	11.5
Super-elastic	$e + Ars \Rightarrow e + Ar$	-11.5
Ionization	$e + Ar \Rightarrow 2e + Ar^+$	15.8
Ionization	$e + Ars \Rightarrow 2e + Ar^+$	4.24
Penning ionization	$Ars + Ars \Rightarrow e + Ar + Ar^+$	-----
Metastable quenching	$Ars + Ar \Rightarrow Ar + Ar$	----

Table 2. Surface reactions.

Reaction	Sticking coefficient
$\mathbf{Ars \Rightarrow Ar}$	1
$\mathbf{Ar^+ \Rightarrow Ar}$	1

4. Governing Equations

As stated above, three species included in the plasma chemistry. The fluid equations of conservation must satisfy for each species separately. For electrons, the density and mean electron energy that solved by COMSOL are :

$$\frac{\partial y}{\partial t}(n_e) + \nabla \cdot [-n_e(\mu_e \cdot E) - D_e \cdot \nabla n_e] = R_e \tag{1}$$

$$\frac{\partial y}{\partial t}(n_\varepsilon) + \nabla \cdot [-n_\varepsilon(\mu_e \cdot E) - D_\varepsilon \cdot \nabla n_\varepsilon] + E \cdot \Gamma_e = R_e \tag{2}$$

where

$$\Gamma_e = -(\mu_e \cdot E)n_e - D_e \cdot \nabla n_e \tag{3}$$

For the electron mobility the COMSOL uses:

$$\mathbf{D}_e = \mu_e T_e \quad , \mathbf{D}_\varepsilon = \mu_\varepsilon T_e \quad , D_\varepsilon = \frac{5}{3}T_e \tag{4}$$

Using plasma chemistry, the source coefficients are determined by Townsend coefficients. The electron source is:

$$R_e = \sum_{j=1}^{M} x_j \alpha_j N_n |\Gamma_e| \tag{5}$$

In which, x_j is the mole fraction of the species for reaction j, N_n is the total neutral number density, α_j is Townsend coefficient for reaction j and Γ_e is electron flux. Summing the collisional energy loss over the entire reactions. And so, the electron energy is:

$$R_\varepsilon = \sum_{j=1}^{P} x_j \alpha_j N_n |\Gamma_e| \Delta\varepsilon_j \tag{6}$$

Such that $\Delta\varepsilon_j$ is the the energy loss from reaction j. For species other than electron the simulation uses:

$$\rho \frac{\partial y}{\partial x}(w_k) + \rho(\boldsymbol{u} \cdot \nabla)w_k = \nabla \cdot \mathbf{j}_k + R_k \tag{7}$$

Where ρ is the space charge density. Equation (8) is used to calculate the electrostatic field

$$-\nabla \cdot \varepsilon_0 \varepsilon_r \nabla V = \rho \qquad (8)$$

Where ρ is calculated using the Equation (9):

$$\rho = q[\textstyle\sum_{k=1}^{N} Z_k n_k - n_e] \qquad (9)$$

Due to the electrons lost to wall by the random motion within some few free paths of the wall, the electrons gained and because the effects of secondary emission there should be a boundary condition (BC) on the energy flux of electron and the flux energy. These BC takes into account in simulation calculations.

3. Results and Discussion

A nearby look at the diagrams provided by COMSOL for the potential, electron and ion density with the separation between anode and cathode would determine the positive column domain. Whatsover point in this domain can be considered as though that the Langmuir probe had been embedded to determine the attributes of the plasma. Thus, this point assigns the calculated data of electron temperature and electron density. The picked point is a few of cm apart from the anode and the other entire computations of plasma parameters are corresponding to this point. Even though the COMSOL draws an electron temperature, electron density, electric potential and excited argon number density along the axial length of the column as well as a surface plot, the latter plots are provided for both electron density over the column of discharge due to various pressures and fixed applied potential and vice versa, elucidate that the electron density is distinctively varied in the glow discharge between the electrodes. In the region between cathode and positive column the electron density decreases rapidly towards the radial direction. This is because of electron diffusive loss outward walls of column. **Figure 1,** shows the electron temperature as a function of applied voltage for several distinct pressures compared with experimental data. Each point in the figure is corresponding to a new run in the COSMOL for the working parameters indicated. Obviously, in the experiment range of measurement, the electron temperature curves against applied voltage decrease for constant pressure. Although, several of COMSOL runs at 0.07 and 0.11 Torr confirm this fact but at the pressure of 0.15 and 0.2 Torr there is fluctuated behavior of increasing and decreasing of electron temperature in slower manner as the applied voltage increased. Note that the peak of each curve is shifted to a lower applied voltage as the pressure increased. Starting from low range of applied voltage, the electron temperature curves for several working pressure have increased behavior reaching behavior to peak and then decreased. The reason of this is that the ionization is effective due to increased probability of electron-neutral collisions. However, as applied voltage increased the elastic collisions prohibit the electrons to attain to the higher energies for the ionization to take place. At higher voltage, these collisions increase the ion loss to the walls yielding to lower electron temperature measured. Notwithstanding that several values of working pressure for the whole range used in the COMSOL do not give common symmetrical curves. The behavior of electron temperature curves with applied voltage is in well agreement with experimental data in [15-16]. The Figure illustrates decreasing values of electron temperature as the working pressure increased.
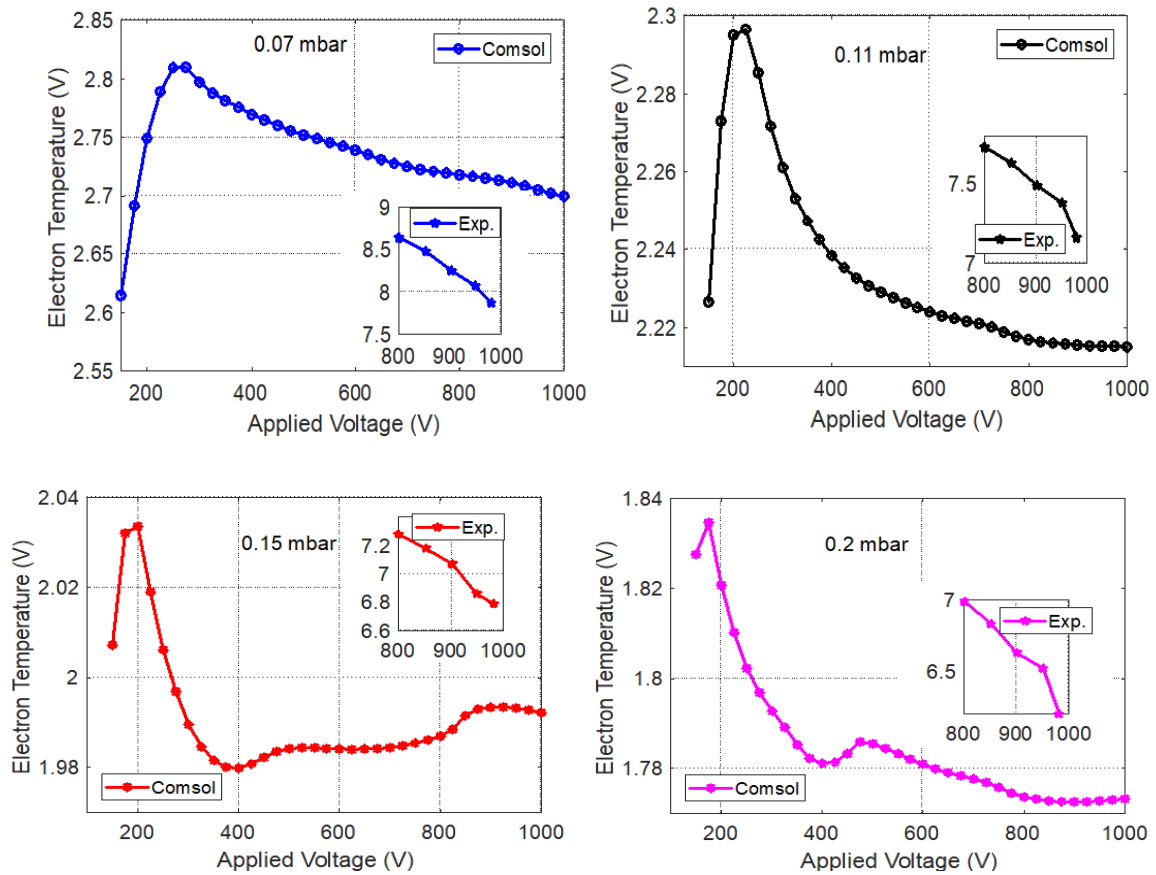
Figure 1. Separated diagrams of calculated and experimental data of electron temperature versus applied potential at different working pressures.

Figure 2, shows the relationship between the electron density and the applied voltage for several values of pressures. Clearly, the electron density increases with the increase of the applied voltage due to the electrons that pick up more energy from the electric field. This process leads to increase the ionization caused by the effect of inelastic collision in the discharge. It is additionally certain that the electron densities for different pressures are very close at lower voltages and its curves diverge as the pressure increased. Further, higher pressures for the same voltages yield higher values of electron density. This originates from the increased ionization within the plasma, which results in an increase in the generation of charged particles. The overall behavior of electron density vs. applied potential in the simulation is in well agreement with experimental data given in [15-16].
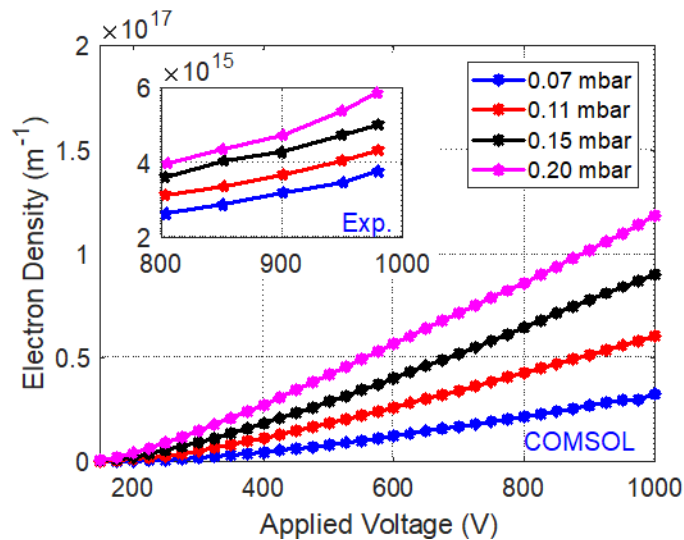
Figure 2. The dependence of electron density on the applied potential at different working pressure.

In **Figure 3,** the impact of the working pressure on electron temperature for many of applied voltages is showed. It is clear that the behavior is exponentially decreasing. At lower voltage used of 150 V, the values of electron temperature are lower than that of higher voltages. It is worth noting that the curve of electron temperature vs. pressure at 250 V and 350 V are approximately located on each other. In fact, the values of electron temperature in the curves are partially different, but they are very close. This causes overlapping of plots and thus we plot the calculations separately. In spite of that, at higher pressures, the electron temperature curves for lower applied voltages are somewhat higher than that of high voltages. This behavior is corresponding to the experimental results in very good manner, see for instant [11-13]. The effect, therefore, means that the electron temperature decreases as the applied voltage increase. The explanation behind the decreasing of electron temperature is the inelastic collision increasing amongst electrons and plasma species. For this situation, electrons do not receive energy from the electric field. It is noted that the curve of electron temperature for applied of 450 V has extremely anomalous behavior at pressure more than 0.13 Torr. It is lying lower than other curves even if the applied voltage increased. This can be caused by the nature of the simulation design in COMSOL. This effect was not observed in the experiment, for example see [11].
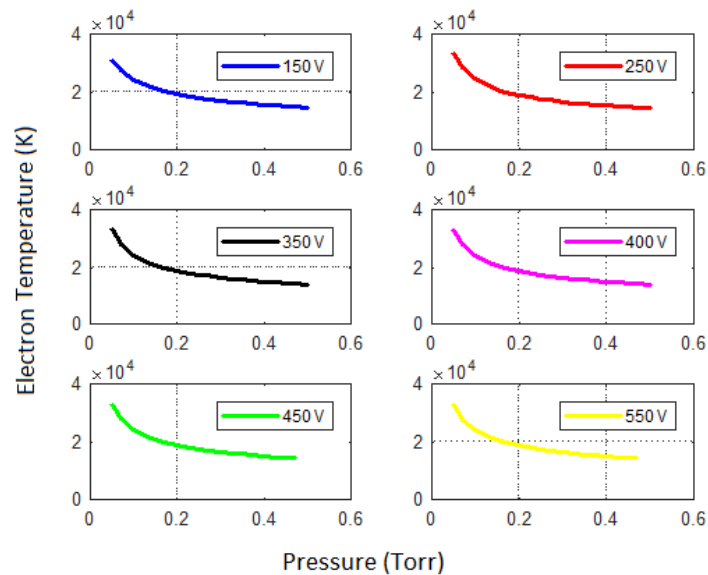
Figure 3. Separated diagrams of electron temperature versus working pressure at different applied potentials.

In **Figure 4,** the reliance of the electron density on working pressure at various applied voltage is showed. As the pressure increases the electron density increased because of the ionization process that is increased in the plasma. Again, it is noticed previously that the electron density increases as the applied pressure increased. However, the simulation results here do not reproduce and match the experimental results of the [11]. There is a direct relationship between the electron density at low pressure values until reaching a peak for certain constant potential and then decreasing. In this simulation, generally the electron density continues to increase at whole range of pressure and applied potential used. The decrease of electron density at higher pressures is not satisfied in the current work. This indicates that the losses of charged particles in the discharge region are as small as the pressure increased. The ionization rate remains to increase and this contribute to the increased electron density.
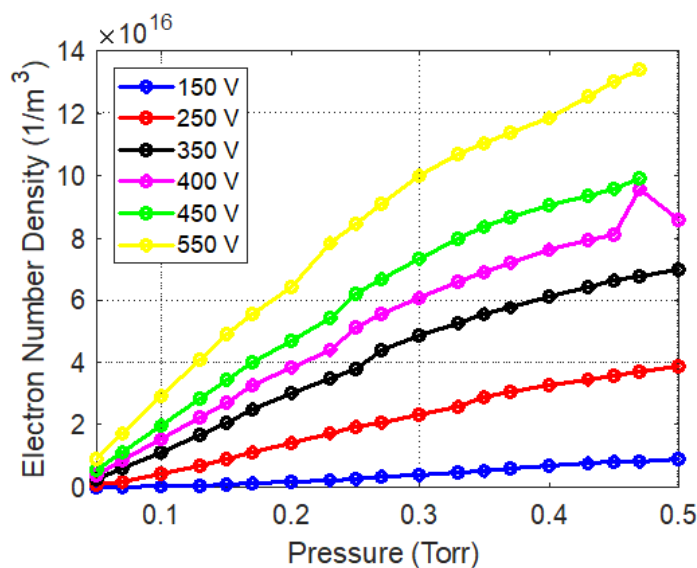

Figure 4. The dependence of electron density on working pressure at various potentials.

In **Figure 5,** gave the dependence of Debye length on the applied potential for different values of applied pressure. The potential of a charged particle penetrates a specific distance in the plasma can be taken as a measure of distance. This distance is a characteristic scale length called Debye length λ_D. The latter is given by well-known expression [17].

$$\lambda_D = \left(\frac{\varepsilon_0 K_B T_e}{n_e e^2}\right)^{1/2} \tag{10}$$

As the applied voltage builds up, the Debye length exponentially decreased. The reason that Debye length decreases is due increasing of electron density that increases the shielding at short distance. Higher applied potential would result in lower curves of Debye length. Higher pressure curve yields lower Debye lengths as one increases the applied pressure. In **Figure 5,** we neglect the lower potential of lower pressures for sake of the other large potential of higher pressures that give shorter Debye length. In this case, the graph is clearer and shows the relationship conceptually. Further, it is clear that the curve of 0.7 Torr is with less data because the COMSOL simulation runs above 375 V fall to give result as previously mentioned. While both the simulation and experimental results of [11]. For the dependence of Debye length on applied voltage has generally decreasing behavior but here is exponential and in the experimental is somehow is linear [11].
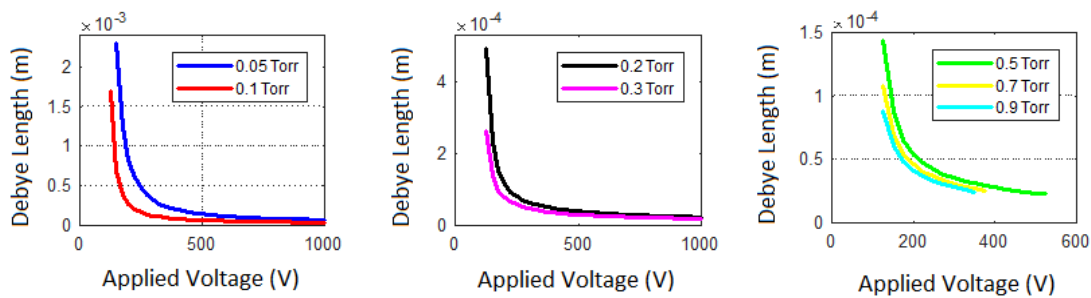

Figure 5. The variation of Debye length with applied potential at different pressure.

Figure 6, demonstrates the Debye length as a function of working pressure for different values of the applied potential. The Debye length decreases as the pressure increased. The curves of higher applied potential results in lower level. The number of particles in the sheath region determines whether the Debye shielding is statistically a valid concept. The Debye shielding is valid provided that there are enough particles in the cloud of charge. The results here are consistent with [11].
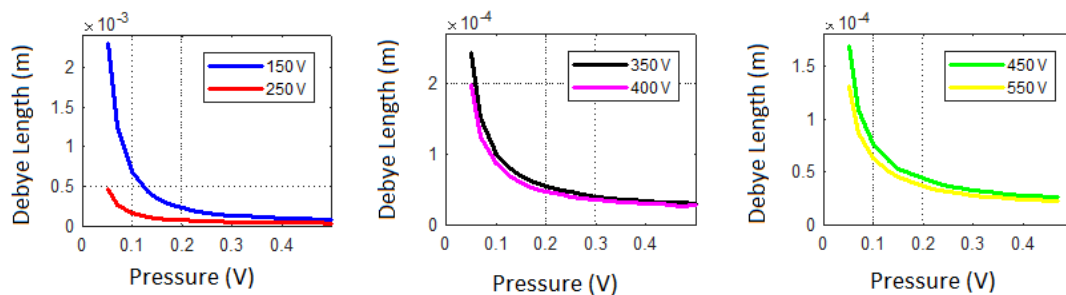

Figure 6. The variation of Debye length with pressure at different applied potentials.

Figure 7, show the dependence of Debye number on the applied voltage for various values of working pressures. The number of particles in a "Debye sphere" is given by [17].

$$N_D = n\frac{4}{3}\pi\lambda_D = 1.38 \times 10^6 T^{3/2} n^{1/2} \ (T \ \text{in} \ ^0\text{K}) \tag{11}$$

Figure 7, illustrate that under a low pressure the positive column of the discharge has less particles than at the higher pressures. As the pressure increases from (0.3 to 0.5) Torr, the corresponding curves of N_D intersect at the point where the applied voltage is 290 V. At relatively lower voltage the N_D curve of 0.3 Torr located lower than 0.5 Torr curve. The curves position is switched after this point. It is additionally evident that when the applied voltage increases, the 0.5 Torr curve will overlap with 0.1 Torr.
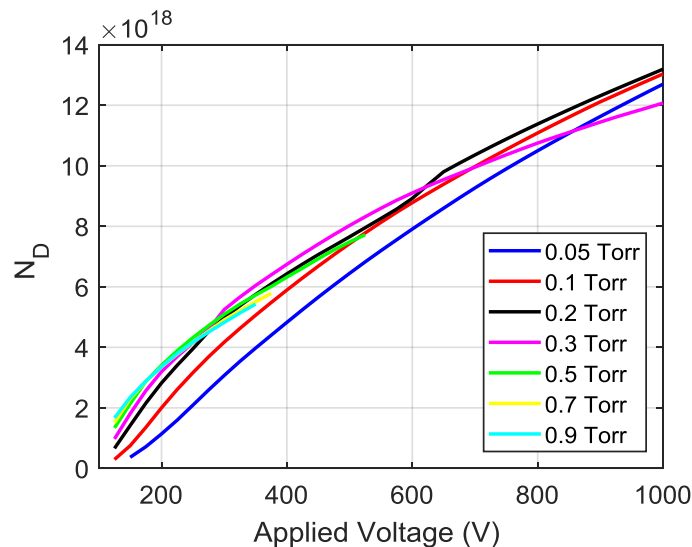

Figure 7. Number of particles in a "Debye sphere" versus applied potential at different pressure.

Figure 8, represents the variation of number of particles with increased applied potentials. It demonstrates that the higher applied voltage gives the most noteworthy number of particles in Debye sphere. The reversal of the N_D of the 350 V curve from increasing to decreasing at higher working pressures. The 250 V curve has a tendency to stabilize in value at higher pressures while the lower voltage used keeps on increasing with increasing pressure.
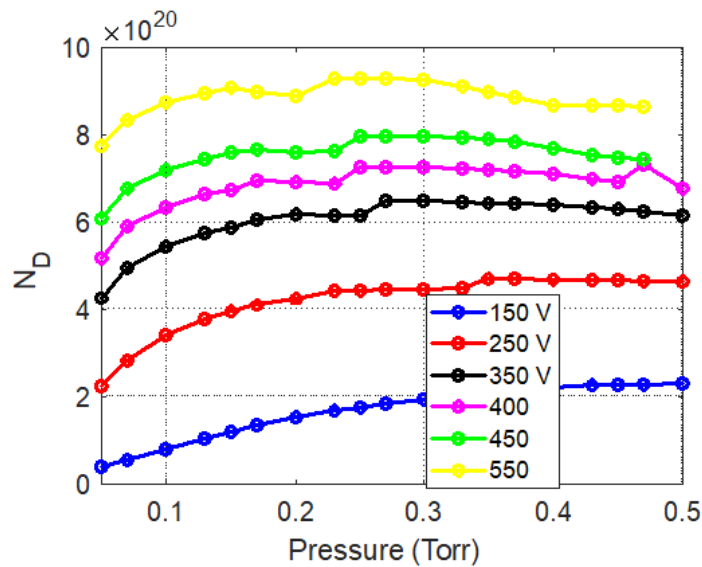
Figure 8. Number of particles in a "Debye sphere" versus pressure at different pressure applied potential

The plasma frequency is one of the fundamental parameters. It depends only on the plasma density since the small value of m_e as in the following formula [17].

$$\omega_p = \left(\frac{n_e e^2}{\varepsilon_0 m_e}\right)^{1/2} \qquad (12)$$

The plasma frequency is normally very high in comparison with an electron frequency. Referable to the increased values of electron density the ω_p behaves in a similar way. **Figure 9,** expresses the variation of a plasma frequency as the applied potential increased for different values of pressure. Evidently, the plasma frequency increases as the applied potential increased and higher pressure yields higher plasma frequency. Compared with the experimental results, we find that the results here are consistent with it in terms of increase in plasma frequency with increasing applied potential [14].
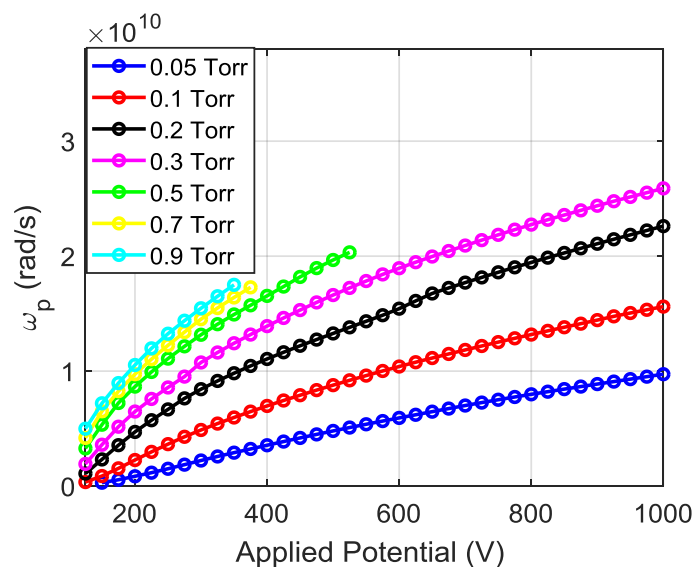

Figure 9. Plasma frequency versus applied potential at different pressure.

Figure 10, illustrate the dependence of plasma frequency with working pressure for different potential. The plasma frequency increases as the pressure increased. Further, the curves of plasma frequency are higher as the applied potential is higher. Once again, it is still that the COMSOL results are contravened with experimental data at higher pressures. The reason is that the plasma frequency behaves as the electron density in **Figure 4**. In fact, plasma frequency is directly proportional with it according to Equation (12).
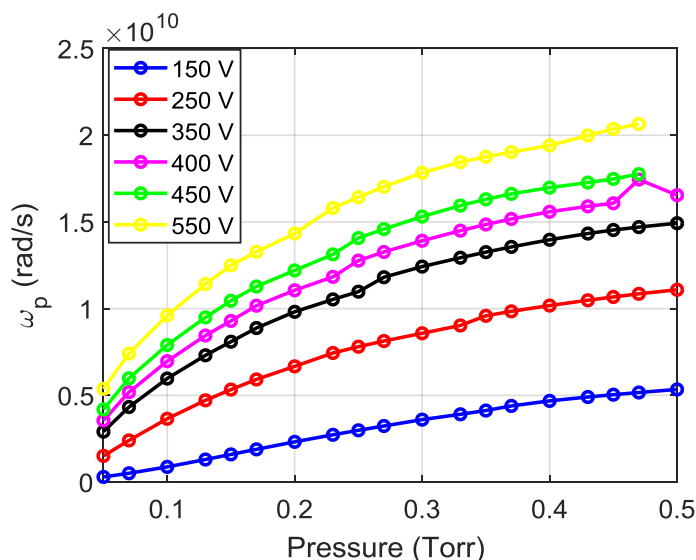

Figure 10. Plasma frequency versus pressure at different pressure applied potential.

4. Conclusion

COMSOL is utilized here to stimulate a dc glow discharge in argon plasma. Generally, the electron temperature progressively decreases with the increase in pressure at constant voltage. However, we indicate that this is not a common case due to COMSOL result for successive close runs. There is increasing in electron temperature at lower pressures and then the behavior returns to the usual. Similar behavior between experimental and COMSOL results for the variation of the electron temperature with the pressure at different applied voltage are obtained. The computed plasma parameters behave like the density and temperature of electron in similar trends depending on its position in the individual formulas applied. The COMSOL results show that they are somehow approved and compatible with experimental data. The difference is the equations used in the COMSOL that must be appropriately formulated to have absolute compatibility with experimental results by considering the boundary conditions at which the difference occurs.

References

1. Guangsup, C.; Lee, J.; Kim, S.; Song, H.; Koo, J.; Kim, B.; Kang, J.; Choi, E.; Lee, U.; Verboncoeur, J. Glow discharge in the external electrode fluorescent lamp, *IEEE Transactions on Plasma Science*.**2005**, *33*,*4*,1410-1415.
2. Kyung, C.; Heung-Sik, T. The Characteristics of Plasma Display with the Cylindrical Hollow Cathode, *IEEE Transactions on Electron Devices*.**1999**, *46*, *12*, 2344-2347.
3. Navaneetha, P.; Selvarjana, V.; Deshmukhb, R.; Changyou, G. Adhesive properties of polypropylene (PP) and polyethylene terephthalate (PET) film surfaces treated by DC glow discharge plasma, *Vacuum*. **2008**, *83*, *2*, 332-339.

4. Gregory, J.F.; Jorge, J.R.A. Self-Consistent Model for Negative Glow Discharge Lasers: The Hollow Cathode Helium Mercury Laser, *IEEE Journal of Quantum Electronics*. **1992**, *28*, *9*, 1941- 1956.

5. Brandenburg, R. Dielectric barrier discharges: progress on plasma sources and on the understanding of regimes and single filaments, *Plasma source science and technology*. **2017**, *26*, *5*, 1-30.

6. Pinheiro, M.J. Electron trapping by electric field reversal in glow discharges, *IST/CFP*. **2006**, *6*, 1-12.

7. Wagenaars, E. Plasma breakdown of low-pressure gas discharges, Ph.D thesis, Eindhoven, University of Technology. **2006**.

8. Samanta, K.; Jassal, M.; Agrawal, A. Atmospheric pressure glow discharge plasma and its applications in textile, *Indian Journal of Fibre and Textile Research*.**2006**, *31*, 83-98.

9. Bengtson, A.; Hoffmann, V.; Kasik, M.; Marshall, K. Analytical Glow Discharges: Fundamentals, Applications, and New Developments, Wiley online library. **2017**.

10. Boumans, P. Sputtering in a glow discharge for spectrochemical analysis. *Anal. Chem*. **1992**, *44*, *7*, 1219–1228.

11. Shrestha, A.; Shrestha, R.; Baniya, H.; Tyata, R.; Subedi, D.; Wong, C. Influence of Discharge Voltage and Pressure on the Plasma Parameters in a Low Pressure DC Glow Discharge. *International Journal of Recent Research and Review*. **2014**, *VII*, *2*, 9-15.

12. Mazhir, S.N.; Khalaf, M.K.; Taha, S.K.; Mohsin, H.K. Measurement of plasma electron temperature and density by using applied voltage and working pressures in a magnetron sputtering system. *International J. of Engineering & Technology*. **2018**, *7*, *3*, 1177-1180.

13. Gao, S.; Chen, S.; Ji, Z.; Tian, W.; Chen, J. DC Glow Discharge in Axial Magnetic Field at Low Pressures. *Advances in Mathematical Physics.* **2017**, Article ID 9193149:1-8.

14. Ali, N.H.; Yeser, M.A.; Ali, N.F. The Effect of the Poles Distances on Plasma Characteristic of Discharge Tube. *Ibn Al-Haitham Journal for Pure and Applied Science*. **2012**, *25*, 1-15.

15. Ali, S. Computational modelling of Dielectric Barrier Discharge Plasma Actuators for Aerospace Flow control applications, M.sc thesis, Delft University of Technology. **2016**.

16. Braithwaite, N. Introduction to gas discharges. *Plasma Sources Sci. Technol*. **2000**, *9*, 517–527.

17. Chen, F. *Introduction to plasma physics and controlled fusion.* Plenum press. 1ˢᵗ edition, **1983**.